FEBS Letters 587 (2013) 2798–2805

FEBS Letters
journal homepage: www.FEBSLetters.org

Establishing catalytic activity on an artificial $(\beta\alpha)_8$-barrel protein designed from identical half-barrels

Josef M. Sperl, Bettina Rohweder, Chitra Rajendran, Reinhard Sterner *

Institute of Biophysics and Physical Biochemistry, University of Regensburg, Universitätsstrasse 31, D-93053 Regensburg, Germany

ARTICLE INFO

Article history:
Received 18 March 2013
Revised 27 May 2013
Accepted 16 June 2013
Available online 24 June 2013

Edited by Christian P. Whitman

Keywords:
Artificial enzyme
Enzyme design
Enzyme evolution
$(\beta\alpha)_8$-Barrel

ABSTRACT

It has been postulated that the ubiquitous $(\beta\alpha)_8$-barrel enzyme fold has evolved by duplication and fusion of an ancestral $(\beta\alpha)_4$-half-barrel. We have previously reconstructed this process in the laboratory by fusing two copies of the C-terminal half-barrel HisF-C of imidazole glycerol phosphate synthase (HisF). The resulting construct HisF-CC was stepwise stabilized to Sym1 and Sym2, which are extremely robust but catalytically inert proteins. Here, we report on the generation of a circular permutant of Sym2 and the establishment of a sugar isomerization reaction on its scaffold. Our results demonstrate that duplication and mutagenesis of $(\beta\alpha)_4$-half-barrels can readily lead to a stable and catalytically active $(\beta\alpha)_8$-barrel enzyme.

1. Introduction

Evolution has provided us with a myriad of enzymes which catalyze an amazing wealth of different reactions with tremendous selectivity and specificity. One of the most important and frequent mechanisms for the creation of new enzymes is the duplication of genes [13,28]. Following duplication, the new gene copy can be either recruited for a new function, or it can be fused with the original gene copy or with another nucleotide fragment from the genome. Especially proteins that exhibit a high degree of internal structure and sequence symmetry suggest a scenario of duplication and fusion of identical gene copies, with a conversion of symmetric oligomers into symmetric monomers [38,53]. However, we can only claim a full understanding of the underlying mechanisms if we are able to build stable and active proteins in the laboratory by reproducing proposed gene duplication and fusion events. Along these lines, recent advances in computational and rational design afforded the creation of stable chimeric proteins by fusing gene fragments from different proteins [10,16,42] or by generating completely artificial proteins from scratch [24]. However, these artificial proteins lacked measurable catalytic activity. In contrast, state-of-the-art computational approaches have allowed for the introduction of new, albeit weak enzymatic activities on existing natural protein scaffolds [19,39,43]. Importantly, these weak activities could be significantly improved by directed laboratory evolution, that is the combination of random mutagenesis with powerful selection or screening techniques [2,22,23,47,48,51].

The $(\beta\alpha)_8$-barrel is one of the oldest, most versatile and ubiquitous protein folds [52]. It is found in about 10% of all proteins with known three-dimensional structure [14]. $(\beta\alpha)_8$-Barrel enzymes can act as oxidoreductases, transferases, lyases, hydrolases and isomerases, thereby covering five of the six enzyme commission (EC) classes. The canonical barrel consists of at least 200 amino acids grouped in eight units. Each unit contains a β-strand which is connected to an α-helix via a βα-loop. The individual modules are linked via αβ-loops. The central barrel is formed by the eight β-strands and surrounded by the eight α-helices. Residuesimportant for substrate specificity and catalysis are found at the C-terminal ends of the β-strands and in the connecting βα-loops whereas the remainder of the structure including the αβ-loops on the opposite face of the barrel are important for stability [45]. The modular structure of the barrel suggests an evolutionary precursor that consisted of $(\beta\alpha)_{n<8}$-modules, and there are multiple hints indicating that modern $(\beta\alpha)_8$-barrels have evolved from $(\beta\alpha)_2$- and $(\beta\alpha)_4$-fragments via gene duplication and fusion events [6,16,25,38]. In particular, the strong fourfold and twofold internal symmetry of the $(\beta\alpha)_8$-barrel enzymes *N*′-[(5′-phosphoribosyl)formimino]-5-aminoimidazole-4-carboxamide ribonucleotide (ProFAR) isomerase (HisA) and imidazole glycerol phosphate synthase (HisF), which

* Corresponding author. Fax: +49 941 943 2813.
E-mail address: reinhard.sterner@ur.de (R. Sterner).

0014-5793/$36.00
http://dx.doi.org/10.1016/j.febslet.2013.06.022

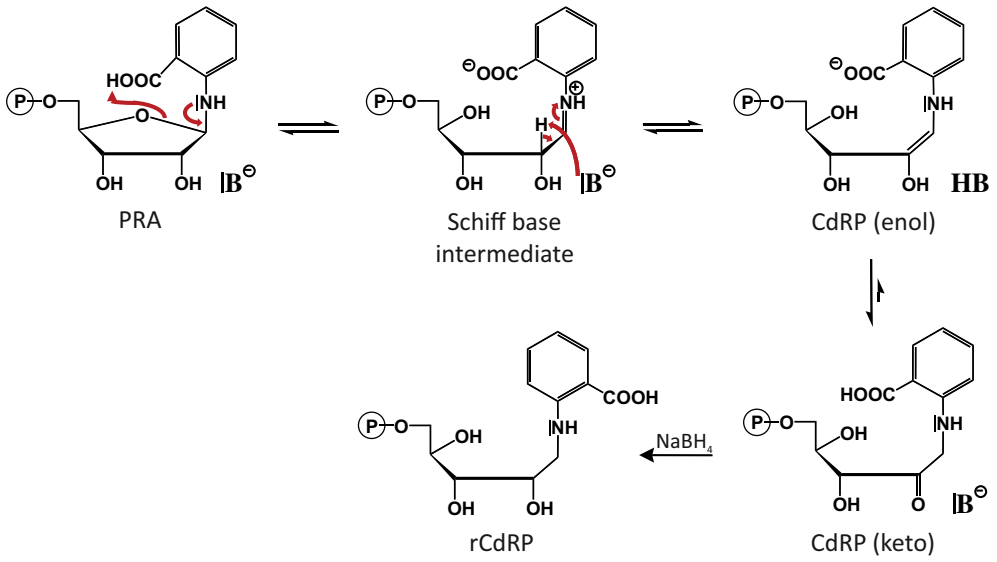

Fig. 1. Scheme for the isomerization of phosphoribosyl anthranilate (PRA) to 1-(2-carboxy-phenylamino)-1′-deoxyribulose-5′-phosphate (CdRP) by HisF-D130V + D176V from *T. maritima*, and the reduction of CdRP to rCdRP by sodium borohydrate ($NaBH_4$). The furanose ring oxygen of PRA is protonated by the carboxylic acid of the anthranilate moiety (substrate assisted catalysis). The proton is most probably transferred via a water molecule (not shown for clarity) [37]. The C2′ atom is then deprotonated by the general base D11 facilitated by the Schiff base intermediate which acts as electron sink. The keto form of CdRP is finally formed by the spontaneous tautomerization of its enolamine form. Reduction of CdRP with sodium borohydrate yields rCdRP.

catalyze two successive steps in histidine biosynthesis, support this scenario [16,27]. We have previously reconstructed the proposed evolutionary process of gene duplication from a $(\beta\alpha)_4$-half-barrel to a $(\beta\alpha)_8$-barrel starting with the C-terminal half of HisF (HisF-C) as a model for the original half-barrel [16,17,40]. Two copies of HisF-C were fused to the HisF-CC construct, which was then stabilized by a combination of rational design and directed evolution, yielding the stable but inactive constructs Sym1 [17] and Sym2 [5].

Here we report on the next and ultimate step of reconstructing $(\beta\alpha)_8$-barrel evolution by establishing enzymatic activity on the artificial $(\beta\alpha)_8$-barrel protein Sym2. As model reaction we used the isomerization of phophoribosyl anthranilate (PRA) to 1-(2-carboxyphenylamino)-1-deoxyribulose-5-phosphate (CdRP), a transformation that is catalyzed by the PRA isomerase (TrpF) within tryptophan biosynthesis (Fig. 1). PRA isomerization is mechanistically rather simple [15,37] and has already been established on several $(\beta\alpha)_8$-barrel enzymes including HisA, HisF [20,26], a HisAF chimera [6], as well as the α-subunit of tryptophan synthase (TrpA) [12]. In a first step, we used rational design to establish binding of reduced CdRP (rCdRP), which is a stable product analog of TrpF. Subsequent to the successful introduction of a high affinity binding pocket for rCdRP on the Sym2 scaffold, random mutagenesis with a very high error rate was performed to create PRA isomerase activity. In vivo selection of variant clones from the resulting library in *trpF*-deficient *Escherichia coli* cells identified an active Sym2 variant that differed from the parental protein at nine amino acid positions. After reducing the number of mutations upon keeping activity, we ended up with a symmetrical construct that contained only six amino acid differences between the two fused $(\beta\alpha)_4$-half-barrels.

2. Materials and methods

2.1. Cloning of Sym2 variants

Cloning of the *sym2* gene into vector pET24a(+) using *Nde*I, *Bam*HI, and *Xho*I restriction enzymes was described previously [5]. For construction of the *sym2_bindC* gene, the 3′-half-sequence of the *sym2* gene, *sym2-C*, was first cloned into plasmid pET24a(+) using BamHI and XhoI restriction sites [5] and mutated at position $D176_C$ by QuikChange™ PCR [50] using the complementary oligonucleotides 5′-CCAGTATCGACAGAGTCGGCACAAA ATCGGG-3′ and 5′-CCCGATTTTGTGCCGACT CTG TCGATACTGG-3′ as overlapping primers (nucleotide exchange underlined), yielding *sym2C-D176V$_C$*. Subsequently, the *sym2C-D130V$_C$* + *D176V$_C$* sequence was amplified by PCR using *sym2C-D176V$_C$* as template. The oligonucleotide 5′-GGTCGC GGATCCCAG GCCGTTGTCGTGGCGA-TAGTTGCAAAAAGAGTGGATGGAGAG-3′ with a BamHI-site at the 5′-terminus (underlined) and a nucleotide exchange (underlined) was used as 5′-primer, and the oligonucleotide 5′-GCTAGT-TATTGCTCAGCGG-3′ was used as 3′-primer. The amplified fragment *sym2C-D130V$_C$* + *D176V$_C$* was cloned into pET24a(+)-sym2 N [5] using *Bam*HI and *Xho*I restriction sites, yielding pET24a(+)-*sym2_bindC*. For construction of the *sym2_bindN* and *sym2_bindNC* genes, the *sym2N-D130V$_N$* + *D176V$_N$* sequence was amplified by PCR using *sym2C-D130V$_C$* + *D176V$_C$* as template. The oligonucleotide 5′-ATACATATGCAGCGCGTT GTCG TGGCGATA-3′ with an *Nde*I-site at the 5′-terminus (underlined) was used as 5′-primer, and the oligonucleotide 5′-CTGGGATCCGAAGGTCTGT-GCGATTTGTGTGATGAGGCTCGGGTTTTCGACAGCGGCAGTATTGATA-GAGACCTTGTCAGCACCTGCCAGGAAG-3′ with a *Bam*HI-site at the 3′-terminus (underlined) was used as 3′-primer. The amplified fragment *sym2N-D130V$_N$* + *D176V$_N$* was cloned into pET24a(+) using *Nde*I and *Bam*HI restriction sites, yielding pET24a(+)-*sym2N-D130V$_N$* + *D176V$_N$*. Next, *sym2-C* and *sym2C-D130V$_C$* + *D176V$_C$* were cloned into pET24a(+)-*sym2N-D130V$_N$* + *D176V$_N$* to yield pET24a(+)-*sym2_bindN* or pET24a(+)-*sym2_bindNC*, respectively. The *cpSym2_bindC* gene was cloned from a modified pTNA plasmid (see below) into a modified pET24a(+) vector using *Sph*I and *Hind*III restriction sites.

2.2. Generation of a plasmid-encoded cpSym2_bindC gene library with randomized N-terminal half

The *cpSym2_bindC* gene was generated and cloned into a modified plasmid, which was derived from pTNA [3,30] and allows for constitutive expression in *E. coli*. The plasmid was constructed in

two steps. First, a *Bsa*I restriction site present in the ampicillin resistance cassette of pTNA was eliminated by QuikChange™ mutagenesis with the complimentary oligonucleotides 5′-GCAATGATACCGCGCGACCCACGCTCACC-3′ and 5′-GGTGAGCGT GGGTCGCGCGGTATCATTGC-3′ as overlapping primers (nucleotide exchanges underlined). Second, the plasmid pET24a(+)-*hisF-D130V + D176V* [37] was used as template for the amplification of the 3′-terminal half-sequence of cpSym2_bindC using 5′-GGCCTCGCATGCAGGGATCCGGTCTCACGACAAGGTGAGCATAAA-CACGGCGGC-3′ as 5′-primer with a *Sph*I-, *Bam*HI- and BsaI-site (underlined) and 5′-CTCTGAAAGCTTAGTGGTGGTGGTGGTGGT-GAGCGTCGGCACCTGCCAGGAAGGCTTCAAGG-3′ as 3′-primer with a *Hind*III-site (underlined). The resulting fragment was cloned into the modified pTNA via *Sph*I and *Hind*III restriction sites, yielding the plasmid pB4. Next, in order to introduce the randomized 5′-terminal half-sequence of cpSym2_bindC, a second *Bsa*I site (underlined) was introduced via the oligonucleotides 5′-CTCGCGGACAAGGTGAGACCG-3′ and 5′-GATCCGGTCTCACCTTGT CCGCGAGCATG-3′, which were mixed and annealed by heating to 95 °C and cooling down to room temperature in a water bath. The annealed oligonucleotides were cloned into pB4 using *Sph*I and *Bam*HI restriction sites to yield pExp-TrpF. The 5′-terminal sequence of *cpSym2_bindC* was subjected to epPCR in 16 reactions with cumulative mutational burden [29]. The first cup contained the template which was the amplification product of a PCR reaction with the oligonucleotide 5′-TCTCCGTG GGGTCTCAAAGGT-GAGCATAAACACGGCGGCTG-3′ with a *Bsa*I-site (underlined) as 5′-primer and the oligonucleotide 5′-AAGCCGCAAGGTCT-CAGTCGGCACCTGCCAGGAAGGCTTC-3′ with a *Bsa*I-site (underlined) as 3′-primer and pET11c(+)-HisF [37] as template. The epPCR reactions with the oligonucleotides 5′-TCTCCGTGGGGT CTCAAAGG-3′ as 5′-primer and 5′- AAGCCGCAAGGTCTCAGTCG-3′ as 3′-primer contained unbalanced concentrations of nucleoside triphosphates (0.2 mM ATP, 0.2 mM GTP, 1 mM CTP, 1 mM TTP), together with 0.5 mM $MnCl_2$ and 5.5 mM $MgCl_2$. After four cycles of amplification 10 µl of the epPCR mixture of the first reaction were transferred to the next cup in order to avoid saturation. This step was repeated until cup 16 was reached [29]. Reactions 7 to 16 were pooled in groups of three and used to purify the amplified fragment. In order to get enough DNA for the cloning step, the PCR products of the four groups were re-amplified in standard PCR reactions. The amplification products were purified from 1% agarose gel. The mixture of randomized genes was then digested with *Bsa*I and the purified reaction products were ligated into the pExp-TrpF plasmid, yielding the *pExp-cpSym2_bindC* library. The ligation reaction was used to transform electro-competent Δ*trpF Escherichia coli* cells [44], which were then streaked out on SOC-plates. The transformants were scraped off using a sterile spatula and liquid LB medium, and the mixture of pExp-cpSym2 library plasmids was prepared from the resulting cell suspension. The size of the gene library was estimated by plating serial dilutions of the transformed cells on small SOC-plates. Size and properties of the resulting gene library are shown in Supplementary Table S1.

2.3. In vivo selection for TrpF-active cpSym2_bindC variants

In vivo complementation to select variants with TrpF activity was performed essentially as described previously [6].

2.4. Analysis of beneficial mutations

In order to replace each of the accumulated mutations individually by the wild-type sequence, the 5′-terminal half-sequence of cpSym2_sel was synthesized by GeneArt™ and subcloned via blunt-ligation into a pUC19-derived vector. Subsequently, each nucleotide exchange with regard to wild-type sequence was reverted separately by QuikChange™ mutagenesis. The resulting nine constructs were then cloned into pExp-TrpF via *Bsa*I restriction sites and tested for their ability to confer growth to Δ*trpF E. coli* cells.

2.5. Cloning of cpSym2_TrpF

We initially cloned the gene for the N-terminal half-barrel of cpSym2_TrpF via blunt-end ligation into a pUC19-derived vector, followed by several steps of QuikChange™ mutagenesis to incorporate the mutations S101I, V140A, T171A and D176G. The resulting construct was then cloned into pExp-TrpF via *Bsa*I restriction sites. The assembled full-length gene was finally subcloned via *Sph*I and *Hind*III restriction sites into a modified pET24a(+)-vector or the pQE70-vector to allow for expression in *E. coli* T7-Express cells (New England Biolabs) or Δ*trpF E. coli* cells, respectively.

2.6. Expression of genes and purification of recombinant proteins

The genes were expressed in *E. coli* T7-Express cells (New England Biolabs) or Δ*trpF E. coli* cells if contamination with wild-type TrpF should be excluded. After induction with 0.5 mM IPTG, cells were grown for 3 h at 37 °C and harvested. Proteins were purified as described for Sym2 by metal chelate affinity chromatography using the C-terminal His_6-tag [5]. According to SDS–Page, the purity of all proteins was assessed >95%.

2.7. Functional characterization

The TrpF activity of purified cpSym2_TrpF was followed at 25 °C by a fluorimetric assay and analyzed as described [18,46]. The binding of the product analog rCdRP was followed by fluorescence energy transfer and analyzed as described [4,15].

2.8. Crystallization, data collection, and structure determination

Crystallization of cpSym2_TrpF was achieved in 96-well plates (Nunc) using the hanging-drop vapor diffusion method at 291 K and the PEG/Ion Screen™ (Hampton Research). Protein crystals belonging to the space group SG P 1 21 1 grew within 8 days in a drop containing 0.3 µl of 0.2 M Calcium acetate hydrate and 20% (w/v) PEG 3350, mixed with 0.3 µl of protein cpSym2_TrpF (17.9 mg/ml), to which 1 mM rCdRP was added. The drop was equilibrated against 100 µl of reservoir buffer. Crystals were flash-frozen in nylon loops in liquid nitrogen. X-ray diffraction data sets were collected with a PILATUS detector at the PXIII beamline at SLS. The data processing was done using XDS [21] and the data quality assessment was done using phenix.xtriage [1]. Molecular replacement was performed with MOLREP within the CCp4i suite [36] using the published high-resolution structure of Sym2 (PDB: 3OG3) as search model. Initial refinement was performed using REFMAC [32]. The model was further improved in several refinement rounds using automated restrained refinement with the program PHENIX [1] and interactive modeling with Coot [11]. The final model was analyzed using the program MolProbity [7]. Data collection and refinement statistics are shown in Supplementary Table S2.

3. Results and discussion

3.1. Introduction of a high affinity rCdRP binding pocket on the Sym2 scaffold

In a first step to establish TrpF activity on the Sym2 scaffold, which is depicted in Fig. 2A, we focused on the introduction of a binding site for the substrate PRA. Since it is difficult to work with

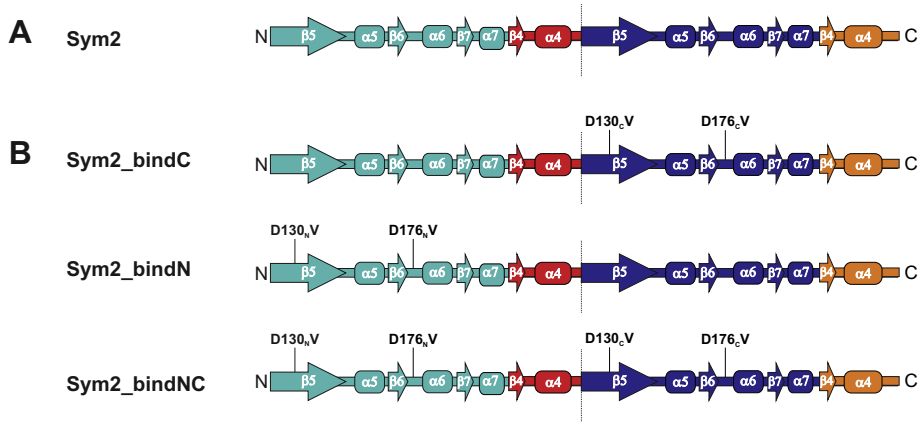

Fig. 2. Design of the artificial $(\beta\alpha)_8$-barrel protein Sym2 and variants thereof that bind rCdRP. (A) Secondary structure elements of Sym2. Parts that stem from the N-terminal half-barrel of HisF are shown in red and orange, parts from the C-terminal half-barrel are shown in turquoise and blue. (B) Design of Sym2 variants. Mutations that impart binding of rCdRP are indicated.

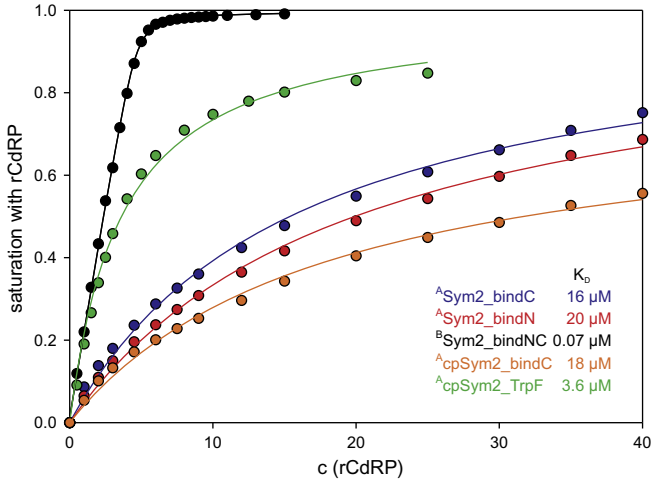

Fig. 3. Analysis of rCdRP binding. Ligand was titrated to 5 µM Sym2_bindC, Sym2_bindN, Sym2_bindNC, and cpSym2_TrpF, and the change in fluorescence emission at 320 nm after excitation at 280 nm was recorded. Reaction conditions: 50 mM Tris–HCl, pH 7.5, 25 °C. Data were fitted to a hyperbolic (A) or quadratic (B) function, and the determined values for the thermodynamic dissociation constants (K_D) are shown.

the labile PRA molecule itself, we decided to generate a binding pocket for rCdRP, which is a structurally similar and stable product analog (Fig. 1). We knew from previous experiments that *Thermotoga maritima* HisF variants D130V and D176V show high affinities for rCdRP with thermodynamic dissociation constants (K_D) of about 0.2 µM [37]. Therefore, we constructed three variants in which we introduced these exchanges in either the N- or the C-terminal half (Sym2_bindN, Sym2_bindC), or in both halves (Sym2_bindNC) of Sym2 (Fig. 2B). In contrast to Sym2, which does not bind rCdRP, both Sym2_bindN and Sym2_bindC have reasonable affinities for rCdRP with K_D values of 16 µM and 20 µM, respectively (Fig. 3). Remarkably, the simultaneous introduction of the D130V and D176V exchanges in both halves resulted in a 250-fold increased affinity, yielding a K_D-value for Sym2_bindNC of 70 nM (Fig. 3). Encouraged by these results we tested whether the three variants have the capacity to catalyze the TrpF reaction in vivo as well as in vitro, but all turned out to be inactive. Nevertheless, the successful rational design of a high-affinity binding pocket for the product analog rCdRP provided us with a starting point for the generation of PRA isomerization activity through random mutagenesis.

3.2. Activation of a circularly permutated variant of Sym2

Due to the high degree of internal symmetry in Sym2 and its three rCdRP-binding competent variants it was not possible to perform random mutagenesis with the entire genes. PCR amplification would predominantly yield half-barrel genes due to duplicate priming sites. Thus, we decided to randomize only one of the two half-barrels and recombine it with the second, non-randomized half. In order to find the most suitable construct for randomization we compared the sequences and structures of our three Sym2 variants with HisF-D130V + D176V. This variant does not only bind rCdRP, but also catalyzes the PRA isomerization reaction [37]. Figs. 2 and 4 show that only Sym2_bindC shares a complete $(\beta\alpha)_4$-unit with HisF-D130V + D176V. Therefore, we decided to insert mutations in Sym2_bindC, however only in those four βα-units which differ from HisF-D130V + D176V. Moreover, for ease of cloning we performed a circular permutation, a step that is also used by natural evolution [35,49], resulting in the construct cpSym2_bindC (Fig. 4). In order to test whether circular permutation changed the functional properties, cpSym2_bindC was produced and its affinity for rCdRP was quantified (Fig. 3). Remarkably, the determined K_D^{rCdRP} of 18 µM is practically identical to the K_D^{rCdRP} values of Sym2_bindN and Sym2_bindC (Fig. 3). The first half of cpSym2_bindC was randomly mutated via error-prone PCR (epPCR). We used a high mutation rate with an average of 12 nucleotide exchanges per half-barrel gene as we wanted to sample as many combinations of amino acid substitutions as possible. Usually, such a high mutagenesis rate would impair the structure of the protein [8]. However, the Sym2 scaffold has an extremely high stability [5], for which reason we considered the chance of finding activating amino acid exchanges higher than the risk of denaturing the whole protein structure. The amplification products of the error-prone PCR with the first half of cpSym2_bindC were subsequently combined with the second, non-randomized half containing the $D130V_C$ and $D176V_C$ exchanges (Fig. 5A). The entire gene repertoire was cloned into the pTNA plasmid [3], and used to transform electro-competent *E. coli* cells. The resulting cpSym2_bindC gene library comprised 5×10^6 independent variants. Taking into account that 42% of the variants contain a stop codon and thus are truncated, non-functional protein, approximately 2×10^6 potentially folded variants remained (Supplementary Table S1). To select for functional variants in our cpSym2_bindC library we used an auxotrophic Δ*trpF E. coli* strain which lacks the ability to synthesize tryptophan [44]. Subsequent to the transformation of Δ*trpF* cells with the cpSym2_bindC library we identified a single variant featuring PRA isomerization activity, by its ability to

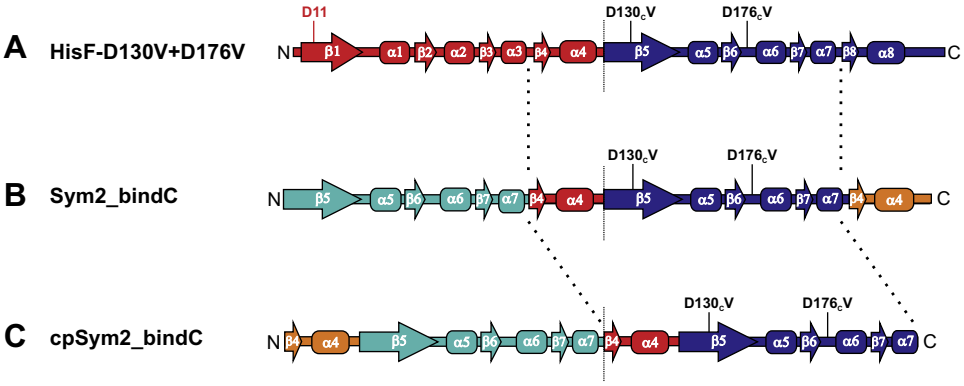

Fig. 4. Design of the starting construct for random mutagenesis cpSym2_bindC. (A) TrpF-active HisF variant HisF-D130V + D176V. The N-terminal half-barrel is shown in red together with residue D11 which acts as general base during catalysis (Fig. 1); the C-terminal half-barrel is shown in blue. Amino acid exchanges leading to PRA isomerization are indicated. (B) rCdRP-binding variant Sym2_bindC shares a complete half-barrel with HisF-D130V + D176V, as indicated by dotted lines. (C) Variant cpSym2_bindC was circularly permutated to facilitate randomization of one half leaving the shared half-barrel untouched.

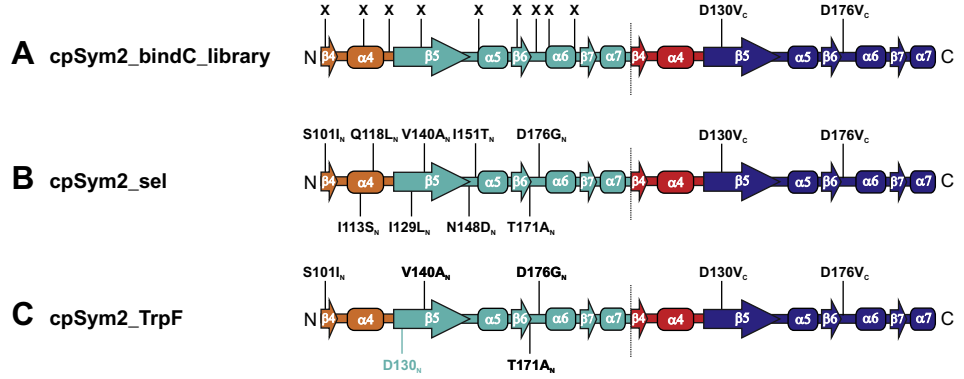

Fig. 5. Library design, selection and amino acid exchanges required for PRA isomerization. (A) Schematic representation of cpSym2 variants in the library. (B) cpSym2_sel was selected by an *in vivo* complementation assay. (C) Four amino acid exchanges (S101I, V140A, T171A, D176G) found in cpSym2_sel are necessary for activity. cpSym2_TrpF which contains only the four required substitutions, shows a high internal symmetry: The N- and C-terminal halves differ at only six amino acid positions. Residue $D130_N$ which acts as general base (Fig. 1) is indicated in cyan.

complement within 6 days the growth deficiency of Δ*trpF* cells on minimal medium. It turned out that the active variant cpSym2_sel accumulated nine additional amino acid substitutions, which are shown in Fig. 5B. Our aim was to generate an active artificial $(\beta\alpha)_8$-barrel with maximum internal symmetry. To this end, each of the nine amino acid exchanges of cpSym2_sel was reversed by site-directed mutagenesis, and the resulting variants were tested for their ability to complement the growth deficiency of the Δ*trpF* strain. The results showed that four substitutions, S101I, V140A, T171A, and D176G, were indispensable for the PRA isomerization reaction. Thus, the approach with an extremely high mutation rate turned out to be crucial since the likelihood of identifying four combined substitutions would have been marginal if we had introduced only a few nucleotide exchanges per gene.

3.3. In vitro PRA isomerization activity of cpSym2_TrpF

Eliminating the five dispensable amino acid exchanges from cpSym2_sel resulted in the final variant cpSym2_TrpF (Fig. 5C). The gene for cpSym2_TrpF was cloned from pTNA into the expression plasmid pET24a(+), and the recombinant protein was produced in *E. coli* and purified by metal chelate affinity chromatography using its C-terminal His_6-tag. The catalytic activity of purified cpSym2_TrpF was tested in vitro by steady-state enzyme kinetics. The analysis of the PRA saturation curve (Fig. 6) with the Michaelis–Menten equation [31] yielded a turnover number (k_{cat}) of 0.07 min^{-1} and a Michaelis constant (K_M^{PRA}) of 7 μM, which is in good accordance with the K_D^{rCdRP} value of 4 μM derived from titration measurements (Fig. 3). Moreover, the catalytic efficiency (k_{cat}/K_M^{PRA}) of 167 $M^{-1}s^{-1}$ obtained for the artificial scaffold cpSym2_TrpF exceeds the (k_{cat}/K_M^{PRA}) of 69 $M^{-1}s^{-1}$ obtained for the natural scaffold HisF-D130V + D176V. However, the catalytic efficiencies of both constructs are lower by about 4–5 orders of magnitude compared to the natural TrpF enzymes from *E. coli* and *T. maritima* (Table 1).

3.4. Crystal structure of cpSym2_TrpF

In order to elucidate the mechanistic basis of PRA isomerization by cpSym2_TrpF we crystallized the protein and solved its X-ray structure at a resolution of 2.3 Å (PDB: 4J9J) Unfortunately, despite the high affinity for rCdRP, we were unable to get a structure of cpSym2_TrpF with bound ligand. However, the liganded structure of HisF-D130V + D176V implied that the PRA isomerization reaction is initiated by the anthranilate moiety of the substrate, which acts as general acid and protonates its own furanose ring oxygen ("substrate-assisted catalysis"). Moreover, D11 acts as the general base which abstracts a proton from the C2′-atom of the Schiff base reaction intermediate [37] (Fig. 1). Assuming a similar mechanism for cpSym2_TrpF, its residue $D130_N$ which corresponds to D11 of HisF-D130V + D176V, would act as general base. Superposition of active cpSym2_TrpF with inactive Sym2 shows that the C-terminal phosphate binding site, which most probably anchors the substrate PRA [6], is shifted by 1.5 Å (residues S201, G202 and G203, Fig. 7A)

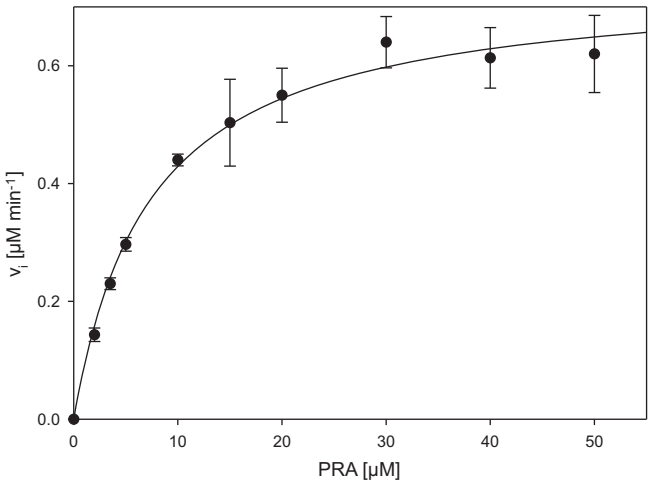

Fig. 6. PRA saturation curve of cpSym2_TrpF. Reaction conditions were 50 mM HEPES pH 7.5, 4 mM EDTA, 4 mM $MgCl_2$, and 2 mM DTT, with PRA concentrations ranging from 2–50 µM. Reactions were performed at 25 °C and initiated by addition of 10 µM cpSym2_TrpF. Values represent the mean and standard deviation of three independent measurements. The solid lines show the result of a hyperbolic fit of the data points, which yielded values for V_{max} of 0.7 µM min^{-1} and for K_M^{PRA} of 7 µM.

Table 1
Steady-state kinetic constants of the PRA isomerization reaction.

Enzyme	k_{cat} (min^{-1})	K_M^{PRA} (µM)	k_{cat}/K_M^{PRA} (M^{-1} s^{-1})
CpSym2_TrpF	0.07 ± 0.02	7 ± 0.7	167
[a]HisF-D130 V + D176 V	0.073	18	69
[b]eTrpF	2070	12.2	2.8×10^6
[c]tTrpF	222	0.28	1.3×10^7

Reaction conditions: 50 mM Hepes, pH 7.5, 4 mM $MgCl_2$, 4 mM EDTA, 2 mM DTT, 25 °C.
[a] Data taken from [37].
[b] Data taken from [18].
[c] Data taken from [46].

due to exchange $S101I_N$. We conclude that this activating amino acid exchange leads to a reorientation of the substrate at the active site which allows for the deprotonation of the Schiff base intermediate by $D130_N$. Moreover, exchanges $V140A_N$ and $T171A_N$ are situated in direct proximity to $D130_N$ thereby changing its environment as well as enhancing its conformational flexibility (Fig. 7B). The non-resolved amino acid exchanges $D176G_N$ and $D176V_C$ as well as $D130V_C$ may facilitate binding of rCdRP through reduction of negative charges in the active center as proposed previously [37].

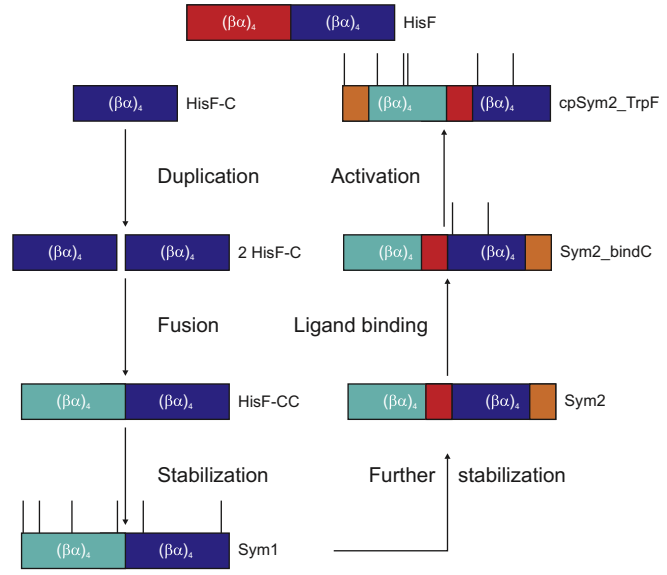

Fig. 8. Schematic overview of laboratory simulation of $(\beta\alpha)_8$-barrel evolution. All evolutionary steps leading from recent HisF to TrpF-active cpSym2_TrpF are shown. Parts are colored according to origin and position (blue: C-terminal half of HisF; red: N-terminal half of HisF; turquoise: C-terminal half after duplication event, now N-terminal; orange: N-terminal half, now C-terminal). Positions of amino acid exchanges leading to respective variants are indicated with lines.

4. Conclusions

Our results represent the ultimate step in our laboratory recreation of $(\beta\alpha)_8$-barrel evolution. By combining rational design with directed evolution techniques, we have gone all the way from duplication of a half-barrel sequence, stabilization of the resulting symmetric protein, introduction of a ligand binding site, and generation of an enzymatically active $(\beta\alpha)_8$-barrel that confers a selective growth advantage (Fig. 8). The success of this simulation has implications for the design and evolution of enzymes in general and of $(\beta\alpha)_8$-barrels in particular. The duplication of existing protein sequences can lead to the emergence of new, robust proteins. The stability of these resulting proteins can be enhanced

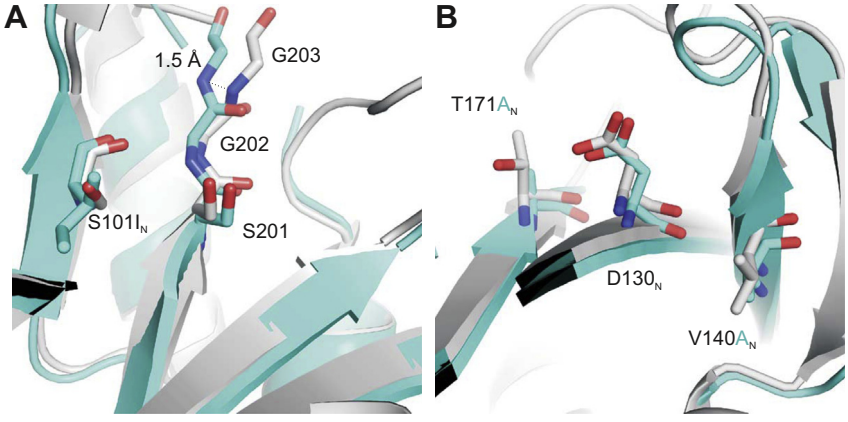

Fig. 7. Structural superposition of cpSym2_TrpF (cyan) with Sym2 (grey). Ribbon diagrams with relevant amino acids are highlighted as sticks. (A) Exchange $S101I_N$ shifts the C-terminal phosphate binding site (residues S201-G203) by 1.5 Å. (B) Exchanges $V140A_N$ and $T171A_N$ are situated in direct proximity to the proposed catalytically active residue $D130_N$ thereby changing its environment.

by directed evolution and screening techniques, or simply by optimizing the cut points at which the sequence was excised from the parental sequence. Once a certain threshold in stability is reached, the sequence can tolerate a high number of mutations without compromising the structure, thus allowing the selection of activating mutations.

Did the natural evolution of the $(\beta\alpha)_8$-barrel fold follow a similar route? We do not know exactly the repertoire of sequences from which nature could choose and whether a recruitment of half-barrels occurred in the natural evolution of the $(\beta\alpha)_8$-barrel fold. However, our findings show that the assembly of two identical half-barrels is a plausible strategy for the evolution of the $(\beta\alpha)_8$-barrel fold and its manifold enzymatic functions. Notwithstanding, the fourfold symmetry of a number of $(\beta\alpha)_8$-barrels suggests that the smallest independently evolving subdomain could have been a quarter-barrel [33]. Along these lines, a computational and experimental analysis indicated that the ancestral half-barrel of HisF was generated by the duplication and fusion of a $(\beta\alpha)_2$-unit [38]. Moreover, the generation of stable and monomeric TrpF fragments comprising $(\beta\alpha)_{1\text{-}5}\beta_6$, and the isolation of similar fragments of triosephosphate isomerase suggests that three-quarter-barrels could also have been intermediates in the evolution of $(\beta\alpha)_8$-barrel proteins [9,41]. In accordance with this hypothesis, the members of the S-adenosyl-L-methionine radical protein family contain not only $(\beta\alpha)_8$-barrel and $(\beta\alpha)_4$ half-barrel but also $(\beta\alpha)_6$-three-quarter barrel structures [34].

Acknowledgements

J.M.S. was supported by a PhD fellowship from the *Fonds der Chemischen Industrie*. We thank Dr. Sandra Schlee for critical reading of the manuscript.

Appendix A. Supplementary data

Supplementary data associated with this article can be found, in the online version, at http://dx.doi.org/10.1016/j.febslet.2013.06.022.

References

[1] Adams, P.D., Grosse-Kunstleve, R.W., Hung, L.W., Ioerger, T.R., McCoy, A.J., Moriarty, N.W., Read, R.J., Sacchettini, J.C., Sauter, N.K. and Terwilliger, T.C. (2002) PHENIX: building new software for automated crystallographic structure determination. Acta Crystallogr., Sect. D: Biol. Crystallogr. 58, 1948–1954.
[2] Althoff, E.A., Wang, L., Jiang, L., Giger, L., Lassila, J.K., Wang, Z.Z., Smith, M., Hari, S., Kast, P., Herschlag, D., et al. (2012) Robust design and optimization of retroaldol enzymes. Protein Sci. 21, 717–726.
[3] Beismann-Driemeyer, S. and Sterner, R. (2001) Imidazole glycerol phosphate synthase from Thermotoga maritima – quaternary structure, steady-state kinetics, and reaction mechanism of the bienzyme complex. J. Biol. Chem. 276, 20387–20396.
[4] Bisswanger, H., Kirschner, K., Cohn, W., Hager, V. and Hansson, E. (1979) *N*-(5-Phosphoribosyl)anthranilate isomerase-indoleglycerol-phosphate synthase.1. Substrate-analog binds to 2 different binding-sites on the bifunctional enzyme from *Escherichia coli*. Biochemistry 18, 5946–5953.
[5] Carstensen, L., Sperl, J.M., Bocola, M., List, F., Schmid, F.X. and Sterner, R. (2012) Conservation of the folding mechanism between designed primordial $(\beta\alpha)_8$-barrel proteins and their modern descendant. J. Am. Chem. Soc. 134, 12786–12791.
[6] Claren, J., Malisi, C., Höcker, B. and Sterner, R. (2009) Establishing wild-type levels of catalytic activity on natural and artificial $(\beta\alpha)_8$-barrel protein scaffolds. Proc. Natl. Acad. Sci. USA 106, 3704–3709.
[7] Davis, I.W., Leaver-Fay, A., Chen, V.B., Block, J.N., Kapral, G.J., Wang, X., Murray, L.W., Arendall, W.B., Snoeyink, J., Richardson, J.S. and Richardson, D.C. (2007) MolProbity: all-atom contacts and structure validation for proteins and nucleic acids. Nucleic Acids Res. 35, W375–W383.
[8] Drummond, D.A., Iverson, B.L., Georgiou, G. and Arnold, F.H. (2005) Why high-error-rate random mutagenesis libraries are enriched in functional and improved proteins. J. Mol. Biol. 350, 806–816.
[9] Eder, J. and Kirschner, K. (1992) Stable substructures of eightfold beta alpha-barrel proteins: fragment complementation of phosphoribosylanthranilate isomerase. Biochemistry 31, 3617–3625.
[10] Eisenbeis, S., Proffitt, W., Coles, M., Truffault, V., Shanmugaratnam, S., Meiler, J. and Höcker, B. (2012) Potential of fragment recombination for rational design of proteins. J. Am. Chem. Soc. 134, 4019–4022.
[11] Emsley, P. and Cowtan, K. (2004) Coot: model-building tools for molecular graphics. Acta Crystallogr., Sect. D: Biol. Crystallogr. 60, 2126–2132.
[12] Evran, S., Telefoncu, A. and Sterner, R. (2012) Directed evolution of $(\beta\alpha)_8$-barrel enzymes: establishing phosphoribosylanthranilate isomerisation activity on the scaffold of the tryptophan synthase α-subunit. Protein Eng. Des. Sel. 25, 285–293.
[13] Fani, R., Mori, E., Tamburini, E. and Lazcano, A. (1998) Evolution of the structure and chromosomal distribution of histidine biosynthetic genes. Origins Life Evol. Biosphere 28, 555–570.
[14] Gerlt, J.A. and Babbitt, P.C. (2001) Barrels in pieces? Nat. Struct. Biol. 8, 5–7.
[15] Henn-Sax, M., Thoma, R., Schmidt, S., Hennig, M., Kirschner, K. and Sterner, R. (2002) Two $(\beta\alpha)_8$-barrel enzymes of histidine and tryptophan biosynthesis have similar reaction mechanisms and common strategies for protecting their labile substrates. Biochemistry 41, 12032–12042.
[16] Höcker, B., Claren, J. and Sterner, R. (2004) Mimicking enzyme evolution by generating new $(\beta\alpha)_8$-barrels from $(\beta\alpha)_4$-half-barrels. Proc. Natl. Acad. Sci. USA 101, 16448–16453.
[17] Höcker, B., Lochner, A., Seitz, T., Claren, J. and Sterner, R. (2009) High-resolution crystal structure of an artificial $(\beta\alpha)_8$-barrel protein designed from identical half-barrels. Biochemistry 48, 1145–1147.
[18] Hommel, U., Eberhard, M. and Kirschner, K. (1995) Phosphoribosyl anthranilate isomerase catalyzes a reversible amadori reaction. Biochemistry 34, 5429–5439.
[19] Jiang, L., Althoff, E.A., Clemente, F.R., Doyle, L., Röthlisberger, D., Zanghellini, A., Gallaher, J.L., Betker, J.L., Tanaka, F., Barbas, C.F., et al. (2008) De novo computational design of retro-aldol enzymes. Science 319, 1387–1391.
[20] Jürgens, C., Strom, A., Wegener, D., Hettwer, S., Wilmanns, M. and Sterner, R. (2000) Directed evolution of a $(\beta\alpha)_8$-barrel enzyme to catalyze related reactions in two different metabolic pathways. Proc. Natl. Acad. Sci. USA 97, 9925–9930.
[21] Kabsch, W. (1993) Automatic Processing of Rotation Diffraction Data from Crystals of Initially Unknown Symmetry and Cell Constants. J. Appl. Crystallogr. 26, 795–800.
[22] Khersonsky, O., Kiss, G., Röthlisberger, D., Dym, O., Albeck, S., Houk, K.N., Baker, D. and Tawfik, D.S. (2012) Bridging the gaps in design methodologies by evolutionary optimization of the stability and proficiency of designed Kemp eliminase KE59. Proc. Natl. Acad. Sci. USA 109, 10358–10363.
[23] Khersonsky, O., Röthlisberger, D., Wollacott, A.M., Murphy, P., Dym, O., Albeck, S., Kiss, G., Houk, K.N., Baker, D. and Tawfik, D.S. (2011) Optimization of the in-silico-designed kemp eliminase ke70 by computational design and directed evolution. J. Mol. Biol. 407, 391–412.
[24] Kuhlman, B., Dantas, G., Ireton, G.C., Varani, G., Stoddard, B.L. and Baker, D. (2003) Design of a novel globular protein fold with atomic-level accuracy. Science 302, 1364–1368.
[25] Lang, D., Thoma, R., Henn-Sax, M., Sterner, R. and Wilmanns, M. (2000) Structural evidence for evolution of the β/α barrel scaffold by gene duplication and fusion. Science 289, 1546–1550.
[26] Leopoldseder, S., Claren, J., Jürgens, C. and Sterner, R. (2004) Interconverting the catalytic activities of $(\beta\alpha)_8$-barrel enzymes from different metabolic pathways: sequence requirements and molecular analysis. J. Mol. Biol. 337, 871–879.
[27] List, F., Sterner, R. and Wilmanns, M. (2011) Related $(\beta\alpha)_8$-barrel proteins in histidine and tryptophan biosynthesis: a paradigm to study enzyme evolution. ChemBioChem 12, 1487–1494.
[28] Lynch, M. and Conery, J.S. (2000) The evolutionary fate and consequences of duplicate genes. Science 290, 1151–1155.
[29] McCullum, E.O., Williams, B.A., Zhang, J. and Chaput, J.C. (2010) Random mutagenesis by error-prone PCR. Methods Mol. Biol. 634, 103–109.
[30] Merz, A., Yee, M.C., Szadkowski, H., Pappenberger, G., Crameri, A., Stemmer, W.P.C., Yanofsky, C. and Kirschner, K. (2000) Improving the catalytic activity of a thermophilic enzyme at low temperatures. Biochemistry 39, 880–889.
[31] Michaelis, L. and Menten, M.L. (1913) Die Kinetik der Invertinwirkung. Biochemische Zeitschrift 49, 333–369.
[32] Murshudov, G.N., Vagin, A.A. and Dodson, E.J. (1997) Refinement of macromolecular structures by the maximum-likelihood method. Acta Crystallogr., Sect. D: Biol. Crystallogr. 53, 240–255.
[33] Nagano, N., Orengo, C.A. and Thornton, J.M. (2002) One fold with many functions: the evolutionary relationships between TIM barrel families based on their sequences, structures and functions. J. Mol. Biol. 321, 741–765.
[34] Nicolet, Y. and Drennan, C.L. (2004) AdoMet radical proteins-from structure to evolution-alignment of divergent protein sequences reveals strong secondary structure element conservation. Nucleic Acids Res. 32, 4015–4025.
[35] Peisajovich, S.G., Rockah, L. and Tawfik, D.S. (2006) Evolution of new protein topologies through multistep gene rearrangements. Nat. Genet. 38, 168–174.
[36] Potterton, L., McNicholas, S., Krissinel, E., Gruber, J., Cowtan, K., Emsley, P., Murshudov, G.N., Cohen, S., Perrakis, A. and Noble, M. (2004) Developments in the CCP4 molecular-graphics project. Acta Crystallogr., Sect. D: Biol. Crystallogr. 60, 2288–2294.
[37] Reisinger, B., Bocola, M., List, F., Claren, J., Rajendran, C. and Sterner, R. (2012) A sugar isomerization reaction established on various $(\beta\alpha)_8$-barrel scaffolds is based on substrate-assisted catalysis. Protein Eng. Des. Sel. 25, 751–760.
[38] Richter, M., Bosnali, M., Carstensen, L., Seitz, T., Durchschlag, H., Blanquart, S., Merkl, R. and Sterner, R. (2010) Computational and experimental evidence for

the evolution of a $(\beta\alpha)_8$-barrel protein from an ancestral quarter-barrel stabilised by disulfide bonds. J. Mol. Biol. 398, 763–773.
[39] Röthlisberger, D., Khersonsky, O., Wollacott, A.M., Jiang, L., DeChancie, J., Betker, J., Gallaher, J.L., Althoff, E.A., Zanghellini, A., Dym, O., et al. (2008) Kemp elimination catalysts by computational enzyme design. Nature 453, 190–U194.
[40] Seitz, T., Bocola, M., Claren, J. and Sterner, R. (2007) Stabillsation of a $(\beta\alpha)_8$-barrel protein designed from identical half barrels. J. Mol. Biol. 372, 114–129.
[41] Setiyaputra, S., Mackay, J.P. and Patrick, W.M. (2011) The structure of a truncated phosphoribosylanthranilate isomerase suggests a unified model for evolution of the $(\beta\alpha)_8$ barrel fold. J. Mol. Biol. 408, 291–303.
[42] Shanmugaratnam, S., Eisenbeis, S. and Höcker, B. (2012) A highly stable protein chimera built from fragments of different folds. Protein Eng. Des. Sel. 25, 699–703.
[43] Siegel, J.B., Zanghellini, A., Lovick, H.M., Kiss, G., Lambert, A.R., Clair, J.L.S., Gallaher, J.L., Hilvert, D., Gelb, M.H., Stoddard, B.L., et al. (2010) Computational design of an enzyme catalyst for a stereoselective bimolecular Diels–Alder reaction. Science 329, 309–313.
[44] Sterner, R., Dahm, A., Darimont, B., Ivens, A., Liebl, W. and Kirschner, K. (1995) $(\beta\alpha)_8$-Barrel proteins of tryptophan biosynthesis in the hyperthermophile thermotoga-maritima. EMBO J. 14, 4395–4402.
[45] Sterner, R. and Höcker, B. (2005) Versatility, stability, and evolution of the $(\beta\alpha)_8$-barrel enzyme fold. Chem. Rev. 105, 4038–4055.
[46] Sterner, R., Kleemann, G.R., Szadkowski, H., Lustig, A., Hennig, M. and Kirschner, K. (1996) Phosphoribosyl anthranilate isomerase from thermotoga maritima is an extremely stable and active homodimer. Protein Sci. 5, 2000–2008.
[47] Sterner, R., Merkl, R. and Raushel, F.M. (2008) Computational design of enzymes. Chem. Biol. 15, 421–423.
[48] Toscano, M.D., Woycechowsky, K.J. and Hilvert, D. (2007) Minimalist active-site redesign: teaching old enzymes new tricks. Angew. Chem., Int. Ed. 46, 3212–3236.
[49] Vogel, C. and Morea, V. (2006) Duplication, divergence and formation of novel protein topologies. BioEssays 28, 973–978.
[50] Wang, W.Y. and Malcolm, B.A. (1999) Two-stage PCR protocol allowing introduction of multiple mutations, deletions and insertions using QuikChange (™) site-directed mutagenesis. Biotechniques 26, 680–682.
[51] Ward, T.R. (2008) Artificial enzymes made to order: Combination of computational design and directed evolution. Angew. Chem., Int. Ed. 47, 7802–7803.
[52] Wierenga, R.K. (2001) The TIM-barrel fold: a versatile framework for efficient enzymes. FEBS Lett. 492, 193–198.
[53] Yadid, I. and Tawfik, D.S. (2007) Reconstruction of functional beta-propeller lectins via homo-oligomeric assembly of shorter fragments. J. Mol. Biol. 365, 10–17.